Volatility by Design. Synthesis and Characterization of Polyether Adducts of Bis(1,1,1,5,5,5-hexafluoro-2,4-pentanedionato)barium and Their Implementation as Metal−Organic Chemical Vapor Deposition Precursors

John A. Belot, Deborah A. Neumayer, Charles J. Reedy, Daniel B. Studebaker, Bruce J. Hinds, Charlotte L. Stern, and Tobin J. Marks*

Department of Chemistry, the Materials Research Center, and the Science and Technology Center for Superconductivity, Northwestern University, Evanston, Illinois 60208-3113

Received January 3, 1997. Revised Manuscript Received April 29, 1997[⊗]

The synthesis and characterization of a series of polyethers and volatile, low-melting polyether complexes of bis(1,1,1,5,5,5-hexafluoro-2,4-pentanedionato)barium having the general formula $Ba(hfa)_2{\cdot}RO(CH_2CH_2O)_nR'$ where R = R′ = CH_3, $n = 3$; R = CH_3, R′ = C_2H_5, $n = 3$; R = R′ = H, $n = 5, 6$; R = R′ = CH_3, $n = 4$; R = CH_3, R′ = C_2H_5, $n = 5$; R = CH_3, R′ = n-C_4H_9, $n = 5, 6$; R = CH_3, R = $C_5H_{11}O$, $n = 3$; R = CH_3, R′ = n-C_6H_{13}, $n = 4, 5$; R = C_2H_5, R′ = n-C_4H_9, $n = 5$; R = n-C_4H_9, R′ = n-C_4H_9, $n = 4, 6$; R = n-C_4H_9, R′ = n-C_6H_{13}, $n = 5$ are reported. The complexes are conveniently synthesized by reaction of n-propylammonium$^+$-hfa$^-$ in DMF with an aqueous solution of $Ba(NO_3)_2$ and the polyether or, alternatively, by reaction of the polyether with $Ba(hfa)_2$ in toluene. These new complexes were characterized by elemental analysis, FT-IR, ^{1}H, ^{13}C, and ^{19}F NMR, MS, X-ray diffraction ($Ba(hfa)_2{\cdot}CH_3O(CH_2CH_2O)_3CH_3{\cdot}H_2O$, $Ba(hfa)_2{\cdot}CH_3O(CH_2CH_2O)_5C_2H_5$), and thermogravimetric analysis. The melting points of the complexes are strongly dependent on the architecture of the polyether chain and dimensions of the terminal polyether substituent, with the lowest melting points corresponding to the longest polyethers having the largest terminal groups. The volatility of the $Ba(hfa)_2{\cdot}$polyether compounds is dependent on molecular weight and molecular structure; however, there is little direct correlation between melting point depression and enhanced volatility. The applicability of these complexes in metal−organic chemical vapor deposition is demonstrated by the successful growth of phase-pure $BaTiO_3$ thin films using $Ba(hfa)_2{\cdot}CH_3O(CH_2CH_2O)_5C_2H_5$ as the Ba source. Phase composition and epitaxy in these films is analyzed by energy-dispersive X-ray spectroscopy and X-ray diffraction $\Theta-2\Theta$, ω, and ϕ scans.

Introduction

Successful metal−organic chemical vapor deposition (MOCVD) of metal oxide ceramics relies on the availability of precursors having high vapor pressures, long-term vapor pressure stability, appropriate reactivity, ease of handling and synthesis, and low cost.[1] Considering these factors, film growth employing metal−organic precursor complexes based on β-diketonate ligands such as dipivaloylmethanate (dpm), acetylacetonate (acac), or 1,1,1,5,5,5-hexafluoropentane-2,5-dionate (hfa) has been achieved with substantial success. However, MOCVD sources utilizing homoleptic β-diketonate coordination complexes of the alkaline earths (notably Ca^{2+}, Sr^{2+}, and Ba^{2+}) have proven to be problematic, being plagued by poorly reproducible stoichiometries, low volatilities, and poor thermal stabilities.[2] These shortcomings reflect, among other factors, the lability and small charge-to-radius ratios of the heavier group II metal ions. The synthesis of sufficiently volatile and stable alkaline earth sources has therefore offered a significant challenge. This paucity of precursors is particularly important given the necessity of incorporating these elements in emerging technologies such as those requiring MOCVD-derived high-temperature superconductor (HTS),[1c,3,4] defect-free ferroelectric,[5] and colossal magnetoresistive[6] thin films.

An effective strategy leading toward superior sources of vapor phase Ca^{2+}, Sr^{2+}, and Ba^{2+} species has been the use of fluorinated ligands such as in $Ba(hfa)_2$[2b,7] (hfa = hexafluoroacetylacetonate), $Ba(fod)_2$[2e,8] (fod = heptafluorodimethyloctanedionate), and $Ba(dfhd)_2$[9] (dfhd = tetradecafluorononadionate). These relatively nonpolar ligands (to reduce lattice cohesive energies/Madelung interactions), with increased steric bulk (to more effectively encapsulate individual M^{2+} ions) and fluorinated groups (to reduce intermolecular van der Waals

[⊗] Abstract published in *Advance ACS Abstracts,* June 15, 1997.

(1) (a) Leedham, T. J. *Mater. Res. Soc. Symp. Proc.* **1996**, *415*, 79. (b) Herrmann, W. A.; Hubert, N. W.; Runte, O. *Angew. Chem., Int. Ed. Engl.* **1995**, *34*, 2187. (c) Marks, T. J. *Pure Appl. Chem.* **1995**, *67*, 313. (d) Schulz, D. L.; Marks, T. J. *Adv. Mater.* **1994**, *6*, 719. (e) Kodas, T.; Hampden-Smith, M. *The Chemistry of Metal CVD*; VCH Publishers: Weinheim, Germany, 1994.

(2) (a) Drake, S. R.; Hursthouse, M. B.; Abdul Malik, K. M.; Otway, D. J. *J. Chem. Soc., Dalton. Trans.* **1993**, 2883. (b) Bradley, D. C.; Hasan, M.; Hursthouse, M. B.; Motevalli, M.; Khan, O. F. Z.; Pritchard, R. G.; Williams, J. O. *J. Chem. Soc., Chem. Commun.* **1992**, 575. (c) Drozdov, A. A.; Trojanov, S. I. *Polyhedron* **1992**, *11*, 2877. (d) Rosetto G.; Polo, A.; Benetollo, F.; Porchia, M.; Zanella, P. *Polyhedron* **1992**, *11*, 979. (e) Turnipseed, S. B.; Barkley, R. M.; Sievers, R. E. *Inorg. Chem.* **1991**, *30*, 1164. (f) Rees, W. S.; Carris M. W.; Hesse, W. *Inorg. Chem.* **1991**, *30*, 4479. (g) Gleizes, A.; Sans-Lenain, S.; Medus, D.; Morancho R. *C. R. l'Academie Sci. Ser. II Univers.* **1991**, *312*, 983. (h) Gardiner, R.; Brown, D. W.; Kirlin P. S.; Rheingold, A. L. *Chem. Mater.* **1991**, *3*, 1053.

S0897-4756(97)00010-0 CCC: $14.00

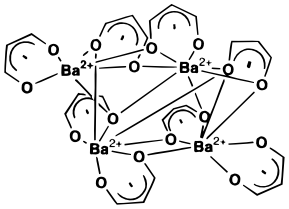

1

Oligomeric
Hygroscopic
Low volatility
Solid sources
Poor thermal stability

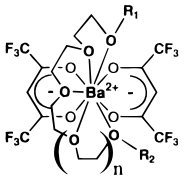

16 - 30

Monomeric
Indefinitely moisture (and air) stable
High, tunable volatility
Liquid barium sources
Excellent thermal stability

Figure 1. Commonly used barium source, $Ba(dpm)_2$ (*tert*-butyl groups not shown), and the newly developed sources, $Ba(hfa)_2$·polyether.

attractions) are more volatile, exhibit more stable vapor pressures, and transport Ba at lower temperatures than the most commonly used hydrocarbon ligand precursor, $Ba(dpm)_2$ (Figure 1, **1**). However, both $Ba(hfa)_2$[7] and $Ba(fod)_2$[8] sublime with decomposition, and $Ba(dfhd)_2$[9] slowly undergoes a structural rearrangement that depresses volatility. A significant improvement over homoleptic fluorinated ligation has been to hinder the decomposition/oligomerization pathways by saturating the metal coordination sphere using neutral Lewis base polyether ligands, such as tetraethyleneglycol dimethyl ether (tet).[10] The resultant $Ba(fluorodiketonate)_2$·polyether complexes (Figure 1, **16**−**30**) are monomeric, volatile, thermally stable with stable vapor pressures, and as is demonstrated here, exhibit "temperature tunable" volatilities and melting points by straightforward modification of the polyether structure.[10e] Indeed, the parent $Ba(hfa)_2$·tet[11] and a number of the new "designer" $Ba(hfa)_2$·polyether complexes have already been successfully implemented in a variety of film growth processes.[12]

Despite the attractive properties of $Ba(hfa)_2$·tet, it has a relatively high melting point of 150 °C, so that it must be sublimed into the reactor feed stream. This characteristic represents a significant deficiency since precursor powders (of any material) have a tendency to sinter and/or shift packing during cycling, greatly altering the available surface area for sublimation and leading to problems associated with unstable vapor pressure and irreproducible film stoichiometry. Therefore, in an effort to reduce the melting point and to develop stable, *liquid Ba MOCVD precursors*[13] (these should provide constant surface areas for evaporation and transport), we initiated a study to synthetically tailor the polyether structures and to explore the properties of the resulting $Ba(hfa)_2$·polyether complexes.[10e,14] In this contribution, we present a full discussion of the properties of $Ba(hfa)_2$·polyether complexes and demonstrate that the melting points and volatilities of these complexes are markedly dependent on the polyether architecture, being tunable via polyether chain length and terminal substituent dimensions. A successful example of this study is $Ba(hfa)_2$·$CH_3O(CH_2CH_2O)_5C_2H_5$ (**23**, Figure 1), a complex that is substantially more volatile than $Ba(hfa)_2$·tet, is a *liquid* under typical film growth conditions, and does not decompose upon repeated thermal cycling. Furthermore, the efficacy of this complex as a viable MOCVD precursor is explicitly demonstrated here by the epitaxial, (100)-oriented growth of films of $BaTiO_3$, a ferroelectric of considerable scientific and technological interest.[5]

Experimental Section

Materials and Methods. The β-diketone H(hfa) (1,1,1,5,5,5-hexafluoro-2,4-pentadione, Genzyme) was distilled before use and handled under N_2. Pyridine (Aldrich, 99+%) was dried and distilled from KOH before use. Heptane (Fisher), toluene, and tetrahydrofuran (THF) were distilled from sodium benzophenone ketyl immediately before use. Distilled, deionized water was used in the synthesis of all Ba complexes. Hexane, dimethylformamide (DMF), *n*-propylamine (98%), tetraethyleneglycol dimethyl ether, triethyleneglycol monomethyl ether (95%), *p*-toluenesulfonyl chloride (98%), 3-methoxy-1-butanol, 2-butoxyethanol, 2-(2-methoxyethoxy)ethanol, 2-(2-ethoxyethoxy)ethanol, 2-(2-butoxyethoxy)ethanol, and 2-(2-hexyloxyethoxy)ethanol were purchased from Aldrich and used as received. Triethylene glycol monobutyl ether, pentaethyleneglycol, and hexaethyleneglycol were purchased from Lancaster and used as received. $Ba(NO_3)_2$ (99.999%, Alfa/AESAR), Ba-

(3) (a) Leskela, M.; Holsa, H.; Niinisto, L. *Superconduct. Sci. Technol.* **1993**, *6*, 627. (b) Tonge, L. M; Richeson, D. S.; Marks, T. J.; Zhao, J.; Zhang, J.; Wessels, B. W.; Marcy, H. O.; Kannewurf, C. R. *Adv. Chem. Ser.* **1990**, *226*, 351.

(4) Shaked, H.; Keane, P. M.; Rodriguez, J. C.; Owen, F. F.; Hitterman, R. L.; Jorgensen, J. D. *Crystal Structures of the High-T_c Superconducting Copper-Oxides*; Elsevier Science B. V.: Amsterdam, The Netherlands, 1994, and references therein.

(5) (a) Kotecki, D. E. *Semiconduct. Int.* **1996**, *19*, 109. (b) Scott, J. F. *Phys. World* **1995**, *2*, 46. (c) Wessels, B. W. *Annu. Rev. Mater. Sci.* **1995**, *25*, 525. (d) Scott, J. F.; Paz de Araujo, C. A. *Science* **1989**, *246*, 1400.

(6) (a) Eckstein, J. N.; Bozovic, I.; O'Donnell, J.; Onellion, M.; Rzchowski, M. S. *Appl. Phys. Lett.* **1996**, *69*, 1312. (b) Rajeswari, M.; Goyal, A.; Raychandhuri, A. K.; Robson, M. C.; Xiong, G. C.; Kwan, C.; Ramesh, R.; Greene, R. L.; Venkatesan, T.; Lakeou, S. *Appl. Phys. Lett.* **1996**, *69*, 851. (c) Fontcuberta, J.; Seffar, A.; Granados, X.; Garcia-Munoz, J. L.; Obradors, X.; Pinol, S. *Appl. Phys. Lett.* **1996**, *68*, 2288. (d) Jin, S.; Teifel, T. H.; McCormack, M.; Fastnacht, R. A.; Ramesh, R.; Chen, L. H. *Science* **1994**, *264*, 413.

(7) Purdy, A. P.; Berry, A. D.; Holm, R. T.; Fatemi, M.; Gaskill, D. K. *Inorg. Chem.* **1989**, *28*, 2799.

(8) (a) Richeson, D. S.; Tonge, L. M.; Zhoa, J.; Zhang, J.; Marcy, H. O.; Marks, T. J.; Wessels, B. W.; Kannewurf, C. R. *Appl. Phys. Lett.* **1989**, *54*, 2145. (b) Zhoa, J.; Dahmen, K. H.; Marcy, H. O.; Tonge, L. M.; Marks, T. J.; Wessels, B. W.; Kannewurf, C. R. *Appl. Phys. Lett.* **1988**, *53*, 1750. (c) Belcher, R.; Cranler, C. R.; Majer, J. R.; Stephen, W. I.; Uden, P. C. *Anal. Chim. Acta* **1972**, *60*, 109.

(9) Thompson, S. C.; Cole-Hamilton, D. J.; Gilliland, D. D.; Hitchman, M. L.; Barnes, J. C. *Adv. Mater. Opt. Electron.* **1992**, *1*, 81.

(10) (a) Motevalli, M.; O'Brien, P.; Watson, I. M. *Polyhedron* **1996**, *15*, 1865. (b) Timmer, K.; Spee, C. I. M. A.; Mackor, A.; Meinema, H. A.; Spek, A. L.; van der Sluis, P. *Inorg. Chim. Acta* **1991**, *190*, 109. (c) Malandrino, G.; Richeson, D. S.; Marks, T. J.; DeGroot, D. C.; Schindler, J. L.; Kannewurf, C. R. *Appl. Phys. Lett.* **1991**, *58*, 182. (d) van der Sluis, P.; Spek, A. L.; Timmer, K.; Meinema, H. A. *Acta Crystallogr.* **1990**, *C46*, 1741. (e) Neumayer, D. A. Ph.D. Thesis, Northwestern University, 1993.

(11) Although the glyme encapsulation strategy has been applied to $Ba(dpm)_2$, the metal center is apparently not sufficiently Lewis acidic to retain the glyme on transport into the vapor phase; see: (a) Drake, S. R.; Miller, S. A. S.; Williams, D. J. *Inorg. Chem.* **1993**, *32*, 3227. (b) Drake, S. R.; Miller, S. A. S.; Hursthouse, M. B.; Abdul Malik, K. M. *Polyhedron* **1993**, *12*, 1621.

(12) For the earliest references, see: (a) Neumayer, D. A.; Schulz, D. L.; Richeson, D. S.; Marks, T. J.; DeGroot, D. C.; Schindler, J. L.; Kannewurf, C. R. *Thin Solid Films* **1992**, *216*, 41. (b) Spee, C. I. M. A.; Vander Zouwen-Assink, E. A.; Timmer, K.; Mackor, A.; Meinema, H. A. *J. Phys. IV* **1991**, *1*, C2/295. (c) Zhang, J. M.; Wessels, B. W.; Richeson, D. S.; Marks, T. J.; DeGroot, D. C.; Kannewurf, C. R. *J. Appl. Phys.* **1991**, *69*, 2743. (d) Duray, S. J.; Buchholz, D. B.; Song, S. N.; Richeson, D. S.; Ketterson, J. B.; Marks, T. J.; Chang, R. P. H. *Appl. Phys. Lett.* **1991**, *59*, 1503. (e) Zhang, J.; Zhao, J.; Marcy, H. O.; Tonge, L. M.; Wessels, B. W.; Marks, T. J.; Kannewurf, C. R. *Appl. Phys. Lett.* **1989**, *54*, 1166.

(13) The application of liquid sources in the MOCVD-mediated growth of high quality $YBa_2Cu_3O_{7-\delta}$ has recently been reported: Yoshida, Y.; Ito, Y.; Hirabayashi, I.; Nagai, H.; Takai, Y. *Appl. Phys. Lett.* **1996**, *69*, 845.

(14) Neumayer, D. A.; Studebaker, D. B.; Hinds, B. J.; Stern, C. L.; Marks, T. J. *Chem. Mater.* **1994**, *6*, 878.

Table 1. Parameters for the Crystal Structure Determinations of Ba(hfa)$_2$·triglyme·H$_2$O (16) and Ba(hfa)$_2$·methylethylpentaglyme (23)

	Ba(hfa)$_2$·triglyme·H$_2$O (**16**)	Ba(hfa)$_2$·methylethylpentaglyme (**23**)
chem formula	$C_{18}H_{22}F_{12}O_9Ba$	$C_{23}H_{30}F_{12}O_{10}Ba$
formula wt	747.68	831.79
crystal color, habit	colorless, columnar	colorless, columnar
crystal dimensions (mm)	0.6 × 0.2 × 0.2	0.4 × 0.18 × 0.14
crystal system	triclinic	triclinic
temp, °C	−120	26
space group	$P\bar{1}$(No. 2)	$P\bar{1}$(No. 2)
a, Å	10.425(2)	11.7383(3)
b, Å	11.476(2)	12.3334(2)
c, Å	13.299(3)	13.0157(3)
α, deg	114.72(1)	69.50(1)
β, deg	96.76(2)	79.909(1)
γ, deg	101.03(2)	74.427(1)
Z value	2	2
d(calc), g cm^{-1}	1.795	1.631
F_{000}	732	824
μ(Mo Kα), cm^{-1}	15.53	12.78
diffractometer	Enraf-Nonius CAD-4	Siemens SMART/CCD
radiation (Mo Kα)	0.710 69 Å	0.710 69 Å
scan type	$\omega-\theta$	ω
$2\theta_{max}$, deg	46.0	56.5
no. of reflns (unique)	3350 (3228, R_{int} = 0.018)	10 908 (7578, R_{int}, 0.032)
intensities > 3.00$\sigma(I)$	3035	5272
corrections	Lorentz-polarization absorption (trans. factors 0.54−0.60) secondary extinction	Lorentz-polarization absorption (trans. factors 0.56−0.79)
no. of parameters	445	633
ρ factor	0.03	0.00
residuals[a] (R; R_w)	0.025; 0.034	0.043; 0.042
GOF	1.88	1.80
diff Fourier, e Å	0.76, −0.83	0.54, −0.41

[a] The definitions for R and R_w are $R = \sum||F_o| - |F_c||/\sum|F_o|$ and $R_w = [(\sum w(|F_o| - |F_c|)^2/\sum wF_o^2)]^{1/2}$.

(hfa)$_2$ (Strem), Ba(dpm)$_2$ (**1**, Strem), and Ti(OC$_2$H$_5$)$_4$ (Gelest) were used as received. Ba(hfa)$_2$·tet was synthesized according to literature procedures.[14,23]

Analytical Methods. Elemental analyses were performed by G. D. Searle (Skokie, IL) or Midwest Microlabs (Indianapolis, IN). NMR spectra were recorded on a Varian Gemini 300 or XL-400 spectrometer with shifts for ^{1}H and ^{13}C referenced to the solvent signal ($CDCl_3$). The ^{19}F chemical shifts are reported relative to $CFCl_3$ in $CDCl_3$. Infrared spectra were recorded on a Mattson Alpha Centauri FTIR using KBr pellets. EI mass spectra were obtained on a VG 70-250 SE spectrometer at 70 eV using a temperature ramp rate of 20 °C/s to 200 °C and were referenced to perfluorokerosene 755. Vacuum TGA data were collected on a TA Instruments SDT 2960 unit at a pressure of 5.00 Torr (±0.05), an N_2 flow of ∼100 sccm, and a temperature ramp of 1.5 °C/min and were analyzed using a previously reported method.[15] Melting points were determined in capillary tubes with a Mel-Temp apparatus and are uncorrected.

Film Growth. Thin films of $BaTiO_3$ were grown using a horizontal quartz, low-pressure MOCVD reactor fitted with external thermostated precursor reservoirs having J. Young isolation valves.[16] The volatile metal sources Ti(OC$_2$H$_5$)$_4$ and **23** were loaded into the reservoirs and independently heated using thermocouple-regulated oil baths. The Ti(OC$_2$H$_5$)$_4$ reservoir temperature was 68 °C with an Ar carrier flow rate of 100 sccm. The barium source, **23**, was maintained at 116 °C with Ar carrier flow rate of 100 sccm. In all depositions, the O_2 oxidant gas was bubbled through H_2O to remove adventitious residual fluorine from the films[3b,17] and was introduced directly upstream of the susceptor at a rate of 100 sccm.

The oxide thin films were deposited on ultrasonically cleaned (acetone) single-crystal (110) $LaAlO_3$ substrates (Applied Technologies, Columbia, SC) secured to a graphite susceptor in the reactor and heated by an infrared lamp (Research Inc., Minneapolis, MN). The (100)-oriented epitaxial $BaTiO_3$ films were grown in situ with a susceptor temperature of 775 °C, 2 h growth time, and a 3.0 Torr total working pressure. Surface morphology and elemental compositions of the MOCVD-derived films were assessed by scanning electron microscopy on a Hitachi S570-LB microscope equipped with a Tracor Northern TN5500 energy-dispersive spectrometer.

X-ray Characterization—Thin Films. Phase purity and preferential growth orientations of the $BaTiO_3$ films were determined using Θ−2Θ, ω, and ϕ scans. The Θ−2Θ patterns were acquired with a computer-interfaced Rigaku DMAX-A instrument using Ni-filtered Cu Kα radiation. The ω-rocking curves of the (200) reflections were acquired with a Spellman double crystal diffractometer having a singly bent LiF monochromator (Cu Kα). The full width at half-maxima of the ω-rocking curves was determined by iterative least-squares fitting. In-plane epitaxy ($b-c$ registry) of the films was determined by ϕ scans on a General Electric diffractometer (18 kW Elliott rotating anode, Cu Kα radiation) with a LiF doubly bent monochromator and a Huber four-circle goniometer.

Single-Crystal Structure Determinations. Single crystals of **16** and **23** were grown by slow evaporation of heptane solutions. Suitable crystals were selected and mounted on glass fibers for data collection. The cell constants and orientation matrix for **16** were obtained by least-squares refinement using setting angles of 25 carefully centered reflections in the range 22.9 < 2Θ < 23.9. A summary of crystallographic data, data collection, refinement parameters, and intensity data options is given in Table 1. The intensity of three representative reflections, which were measured every 90 min of X-ray exposure time, remained constant throughout each data collection, indicative of crystal and electronic stability (no decay correction was applied) for **16**. An analytical absorption correction for **16** was applied, resulting in transmission factors ranging from 0.54 to 0.60, and for **23** an empirical correction was used with maximum and minimum transmission factors

(15) (a) Hinds, B. J.; Studebaker, D. B.; Chen, J.; McNeely, R. J.; Han, B.; Schindler, J. L.; Hogan, T. P.; Kannewurf, C. R.; Marks, T. J. *J. Phys. IV* **1995**, *5*, C5/391. (b) Hinds, B. J.; McNeely, R. J.; Studebaker, D. B.; Marks, T. J.; Hogan, T. P.; Schindler, J. L.; Kannewurf, C. R.; Zhang, X. F.; Miller, D. J. *J. Mater. Res.* **1997**, *12*, 1214.

(16) Hinds, B. J.; Schulz, D. L.; Neumayer, D. A.; Han, B.; Marks, T. J.; Wang, Y. Y.; Dravid, V. P.; Schindler, J. L.; Hogan, T. P.; Kannewurf, C. R. *Appl. Phys. Lett.* **1994**, *65*, 231.

(17) (a) Mizushima, Y.; Hirabayashi, I. *J. Mater. Res.* **1996**, *11*, 2698. (b) Watson, I. M.; Atwood, M. P.; Cardwell, D. A.; Cumberbatch, T. J. *J. Mater. Chem.* **1994**, *4*, 1393.

of 0.5623 and 0.7861, respectively. The data were corrected for Lorentz and polarization effects. A correction for secondary extinction was applied (coefficient = 0.27177E−05) to the data for **16**.

The crystal structure of **16** was solved by direct methods[18] using TEXSAN[19] and SHELXS-86 programs. The non-hydrogen atoms were refined anisotropically except the disordered fluorine atoms (F7−F9, F10−F12). The hydrogen atoms of the coordinated H_2O were refined isotropically. The remaining hydrogen atoms were included as fixed parameters in "idealized" positions. The disordered fluorine atoms refined to site occupancies of 0.574 for F7−F9 and 0.403 for F10−F12. The disordered carbon atoms, C16 and C17, were refined to site occupancies of 0.575. No hydrogen atoms were idealized for the disordered carbon atoms.

The structure of **23** was solved by direct methods[18] using SHELXS-86 and refined using TEXSAN.[19] The non-hydrogen atoms were refined anisotropically, and hydrogen atoms were included but not refined in idealized positions. The CF_3 groups of C22 and C23 were refined to disorder in two positions, with the occupancy of C22, C23, F4−F6, and F7−F9 being 0.425 and that of C22A, C23A, F4A−F6A, and F7A−F9A being 0.575. Similarly, the CF_3 groups of C17 and C18 were disordered over three sites and fixed to 0.33 occupancy.

Tosylation of Monoalkyl Polyethers. *1,4,7,10-Butoxaundecyltosylate (**2**).* In a representative procedure using a 2-L round-bottom flask, 164 g (1.00 mol) of triethylene glycol monomethyl ether was dissolved in 1.0 L of pyridine and cooled to 0 °C. As the solution was mechanically stirred, 194 g (1.00 mol) of *p*-toluenesulfonyl chloride was added over 1 h (in 10−15 g portions), and the reaction mixture stirred overnight during which time it warmed to ambient temperature. The mixture was then poured onto 1 L of ice and acidified to pH = 2 using concentrated HCl. The aqueous layer was extracted four times with 250 mL of diethyl ether, and the combined organics were washed with aqueous sodium carbonate, followed by drying over Na_2SO_4. After filtration, the volatiles were removed in vacuo, yielding 105 g (33%) of yellow liquid. ^{1}H NMR δ 1.39 (s, 3H), 3.32 (s, 3H), 3.48 (m, 2H), 3.57 (m, 6H), 3.66 (m, 2H), 4.10 (m, 2H), 7.31 (d, 2H), 7.77 (d, 2H). Anal. Calcd for $C_{14}H_{22}O_6S$: C, 52.82; H, 6.96. Found: C, 51.77; H, 7.11.

*1,4,7,10-Butoxatetradecyltosylate (**3**).* In a procedure identical with that described above, this synthesis utilized 206 g (1.00 mol) of triethyleneglycol monobutyl ether as starting material. After acidification with concentrated HCl, the aqueous layer was extracted four times with $CHCl_3$, and the combined organics were washed with aqueous sodium carbonate, followed by drying over Na_2SO_4. After filtration, the volatiles were removed in vacuo, yielding 185 g (51%) of yellow liquid. ^{1}H NMR δ 0.87 (m, 3H), 1.31 (m, 2H), 1.52 (m, 2H), 2.41 (s, 3H), 3.41 (m, 2H), 3.55 (s, 10H), 3.65 (m, 2H), 7.30 (d, 2H), 7.76 (d, 2H). Anal. Calcd for $C_{17}H_{28}O_6S$: C, 56.65; H, 7.83. Found: C, 56.38; H, 7.98.

*1,4,7-Propoxatridecyltosylate (**4**).* In a procedure identical with that described for **2**, this synthesis utilized 191 g (1.00 mol) of 2-(2-hexylethoxy)ethanol as starting material. Yield 43% (yellow liquid). ^{1}H NMR δ 0.85 (m, 3H), 1.25 (m, 6H), 1.53 (m, 2H), 2.42 (s, 3H), 3.39 (t, 2H), 3.49 (m, 2H), 3.54 (m, 2H), 3.66 (m, 2H), 4.14 (m, 2H), 7.30 (d, 2H), 7.76 (d, 2H). Anal. Calcd for $C_{17}H_{24}O_5S$: C, 60.00; H, 7.06. Found: C, 59.48; H, 7.75.

Polyether Synthesis. *2,5,8,11-Tetraoxatridecane:Triethyleneglycol Methylethyl Ether (**5**).* This synthesis followed a modified literature procedure.[20] Under N_2, 20 g (0.12 mol) of triethyleneglycol monomethyl ether was added dropwise over 1 h to a stirring suspension of 3.2 g (0.14 mol) of NaH and 500 mL of DMF (dried and distilled from BaO). After 1 h of stirring, 14.6 g (0.134 mol) of ethyl bromide was added dropwise, and the reaction allowed to continue for 24 h. The DMF was then removed in vacuo, and the crude product vacuum distilled from the remaining NaBr. The crude product was then added dropwise to a stirring suspension of 3.3 g (0.14 mol) of NaH and 500 mL of DMF, and stirring continued for 1 h, after which time 14.6 g (0.134 mol) of ethyl bromide was added. The reaction was then stirred for an additional 24 h, the DMF removed in vacuo, and the yellow oil diluted with diethyl ether and extracted with water. The remaining organics were dried over $MgSO_4$ and filtered, and the solvent was removed in vacuo. The crude product was distilled (bp 77−80 °C/10^{-2} Torr) from BaO yielding 15.7 g (68%) of product as a colorless liquid. ^{1}H NMR δ 1.14 (m, 3H), 3.31 (s, 3H), 3.45 (m, 2H), 3.49 (m, 2H), 3.53 (m, 2H), 3.58 (m, 2H), 3.61 (s, 6H). ^{13}C NMR δ 14.8, 58.5, 66.1, 69.4, 70.05, 70.13, 70.15, 71.5. Anal. Calcd for $C_9H_{20}O_4$: C, 56.23; H, 10.48. Found: C, 55.97; H, 10.77.

*2,5,8,11,15-Pentaoxa-14-methylhexadecane:Triethyleneglycol 2-Methoxybutyl Methyl Ether (**6**).* Under N_2, 13.3 g (0.128 mol) of 3-methoxy-1-butanol was added dropwise over 1 h to a stirring suspension of 2.9 g (0.12 mol) of NaH and 500 mL of THF. After 1 h, 34.0 g (0.107 mol) of **2** was added dropwise, and stirring continued for 24 h. The reaction mixture was then filtered, the volatiles removed in vacuo, and the crude product distilled (82−85 °C/10^{-2} Torr) affording 13.6 g (51%) of product as a colorless oil. ^{1}H NMR δ 1.10 (d, 3H), 1.70 (m, 2H), 3.27 (s, 3H), 3.33 (s, 3H), 3.42 (m, 1H), 3.50 (m, 4H), 3.54 (m, 2H), 3.60 (m, 4H), 3.62 (s, 4H). ^{13}C NMR δ 18.5, 35.9, 55.27, 55.33, 58.2, 67.2, 69.5, 69.9, 71.2, 73.2. Anal. Calcd for $C_{12}H_{26}O_5$: C, 57.58; H, 10.47. Found: C, 57.42; H, 10.93.

*5,8,11,14,17-Pentaoxauneicosane:Tetraethyleneglycol Dibutyl Ether (**7**).* Under N_2, 5.6 g (0.048 mol) of 2-butoxyethanol was added dropwise over 1 h to a stirring suspension of 1.4 g (0.053 mol) of NaH in 500 mL of THF. After 1 h, 19.1 g (0.0568 mol) of **3** was added dropwise, and stirring continued for 24 h. The reaction was then filtered, the volatiles were removed in vacuo, and the crude product was distilled twice (142 °C/1.0 Torr), affording 5.6 g (38%) of product as a colorless liquid. ^{1}H NMR δ 0.87 (t, 6H), 1.31 (m, 4H), 1.52 (m, 4H), 3.41 (t, 4H), 3.54 (m, 4H), 3.61 (s, 12H). ^{13}C NMR δ 13.74, 19.07, 31.52, 69.88, 70.41, 70.96. Anal. Calcd for $C_{16}H_{34}O_5$: C, 62.71; H, 11.18. Found: C, 62.65; H, 10.88.

*2,5,8,11,14-Hexaoxaeicosane:Tetraethyleneglycol Methylhexyl Ether (**8**).* Under N_2, 7.2 g (0.060 mol) of 2-(2-methoxyethoxy)-ethanol was added dropwise over 20 min to a rapidly stirring suspension of 1.2 g (0.052 mol) of NaH and 500 mL of THF in a 1 L flask. After the addition was complete, 17.7 g (0.0546 mol) of **4** was added dropwise. The red-brown solution was stirred for 24 h, and the THF then removed in vacuo. The crude product was distilled twice (bp 121 °C/0.1 Torr) to yield 9.87 g (67%) of product as a yellow oil. ^{1}H NMR δ 0.84 (t, 3H), 1.25 (m, 6H), 1.53 (m, 2H), 3.34 (s, 3H), 3.40 (t, 2H), 3.52 (m, 4H), 3.62 (s, 12H). ^{13}C NMR δ 13.21, 21.77, 24.96, 28.79, 30.87, 57.95, 69.26, 69.75, 70.48, 71.09. Anal. Calcd for $C_{15}H_{32}O_5$: C, 61.61; H, 11.03. Found: C, 61.29; H, 10.91.

*2,5,8,11,14,17-Hexaoxanonadecane:Pentaethyleneglycol Methylethyl Ether (**9**).* Under N_2, 10.2 g (0.0761 mol) of 2-(2-ethoxyethoxy)ethanol was added dropwise over 1 h to a rapidly stirring suspension of 1.9 g (0.079 mol) of NaH and 500 mL of THF. After the addition was complete, 24.4 g (0.0767 mol) of **2** was added dropwise. Stirring was continued for 24 h at room temperature, the reaction mixture was then filtered, and the volatiles were removed in vacuo. The crude product was distilled twice (bp 122−125 °C/0.01 Torr) yielding 15.6 g (72%) of product as a colorless oil. ^{1}H NMR δ 1.12 (t, 3H), 3.30 (s, 3H), 3.40−3.65 (m, 22H). ^{13}C NMR δ 14.5, 58.2, 65.7, 69.1, 69.8, 71.2. Anal. Calcd for $C_{13}H_{28}O_6$: C, 55.70; H, 10.07. Found: C, 55.16; H, 10.10.

*2,5,8,11,14,17-Hexaoxauneicosane:Pentaethyleneglycol Methylbutyl Ether (**10**).* Under N_2, 16.2 g (0.100 mol) of 2-(2-butoxyethoxy)ethanol was added dropwise over 1 h to a rapidly stirring suspension of 2.4 g (0.10 mol) of NaH and 500 mL of THF in a 1 L flask. After the addition was complete, 31.8 g (0.100 mol) of **2** was added dropwise. Stirring was continued at room temperature for 24 h, the reaction mixture was filtered, and the volatiles were removed in vacuo. The crude product was distilled twice (bp 155 °C/1.0 Torr) affording 22.4 g (73%) of product as a colorless liquid. ^{1}H NMR δ 0.86 (t,

(18) DIRDIF94: Beurskens, P. T.; Admiraal, G.; Beurskens, G.; Bosman, W. P.; de Gelder, R.; Israel, R.; Smits, J. M. M., 1994. The DIRDIF-94 program system, Technical Report of the Crystallography Laboratory, University of Nijmegen, Netherlands.

(19) TEXSAN, Texray Structural Analysis Package, Molecular Structure Corp.: The Woodlands, TX.

(20) Vogel, A. I. *J. Am. Chem. Soc.* **1948**, *70*, 616.

3H), 1.31 (m, 2H), 1.51 (m, 2H), 3.33 (m, 3H), 3.40 (t, 2H), 3.52 (m, 4H), 3.61 (s, 16H). ^{13}C NMR δ 13.86, 19.18, 31.60, 58.93, 69.96, 70.48, 71.10, 71.82. Anal. Calcd for $C_{15}H_{32}O_6$: C, 58.42; H, 10.46. Found: C, 57.84; H, 10.47.

*2,5,8,11,14,17-Hexaoxatricosane:Pentaethyleneglycol Methylhexyl Ether (**11**).* Under N_2, 7.2 g (0.044 mol) of triethylene glycol monomethyl ether was added dropwise to a rapidly stirring suspension of 1.2 g (0.050 mol) of NaH in 500 mL of THF in a 1 L flask. After the addition was complete, 17.7 g (0.0514 mol) of **4** was added dropwise. The reaction mixture was allowed to stir for 24 h and filtered, and the volatiles were removed in vacuo. The crude product was distilled twice (bp 139 °C/0.08 Torr) yielding 9.9 g (68%) of product as a yellow liquid. ^{1}H NMR δ 0.84 (t, 3H), 1.25 (m, 6H), 1.54 (m, 2H), 3.34 (s, 3H), 3.41 (t, 2H), 3.53 (m, 4H), 3.62 (s, 16H). ^{13}C NMR δ 13.51, 22.07, 25.24, 29.07, 31.15, 58.42, 69.55, 70.05, 70.90, 71.39. Anal. Calcd for $C_{17}H_{36}O_6$: C, 60.69; H, 10.78. Found: C, 60.62; H, 10.64.

*3,6,9,12,15,18-Hexaoxadocosane:Pentaethyleneglycol Ethylbutyl Ether (**12**).* Under N_2, 6.3 g (0.047 mol) of 2-(2-ethoxyethoxy)ethanol was added dropwise to a rapidly stirring suspension of 1.2 g (0.050 mol) of NaH and 500 mL of THF in a 1 L flask. After the addition was complete, 15.5 g (0.0431 mol) of **3** was added dropwise. The reaction mixture was allowed to stir for 24 h and filtered, and the volatiles were removed in vacuo. The crude product was distilled (bp 152 °C/1.0 Torr) yielding 4.9 g (35%) of product as a colorless liquid. ^{1}H NMR δ 0.85 (t, 3H), 1.15 (t, 3H), 1.30 (m, 2H), 1.51 (m, 2H), 3.43 (m, 4H), 3.53 (m, 4H), 3.60 (s, 16H). ^{13}C NMR δ 12.92, 14.17, 18.28, 30.77, 68.87, 69.12, 69.59, 69.98. Anal. Calcd for $C_{16}H_{34}O_6$: C, 59.60; H, 10.63. Found: C, 59.02; H, 10.82.

*5,8,11,14,17,20-Hexaoxahexacosane:Pentaethyleneglycol Butylhexyl Ether (**13**).* Under N_2, 8.4 g (0.044 mol) of 2-(2-hexyloxyethoxy)ethanol was added dropwise to a rapidly stirring suspension of 1.2 g (0.050 mol) of NaH and 200 mL of THF in a 500 mL flask. After the addition was complete, 18.7 g (0.0519 mol) of **3** was added dropwise. The reaction mixture was allowed to stir for 24 h and filtered, and the volatiles were removed in vacuo. The crude product was distilled (bp 170 °C/0.05 Torr) yielding 7.3 g (44%) of product as a colorless liquid. ^{1}H NMR δ 0.86 (m, 6H), 1.29 (m, 8H), 1.52 (m, 4H), 3.41 (m, 4H), 3.54 (m, 4H), 3.62 (s, 16H). ^{13}C NMR δ 13.59, 13.71, 18.90, 22.29, 25.46, 29.28, 31.39, 69.76, 70.26, 70.75, 71.15.

*2,5,8,11,14,17,20-Heptaoxatetracosane:Hexaethyleneglycol Methylbutyl Ether (**14**).* Under N_2, 18.3 g (0.0888 mol) of triethyleneglycol monobutyl ether was added dropwise to a rapidly stirring suspension of 2.1 g (0.088 mol) of NaH and 500 mL of THF. After the addition was complete, 28.3 g (0.0890 mol) of **2** was added dropwise. The reaction mixture was allowed to stir for 24 h and filtered, and the volatiles were removed in vacuo. The crude product was distilled twice (bp 163−5 °C/10^{-2} Torr) yielding 21.4 g (70%) of product as a colorless liquid. ^{1}H NMR δ 0.87 (m, 3H), 1.32 (m, 2H), 1.53 (m, 2H), 3.34 (s, 3H), 3.42 (m, 2H), 3.51 (m, 2H), 3.55 (m, 2H), 3.61 (s, 20H). ^{13}C NMR δ 13.4, 18.7, 31.1, 58.3, 58.4, 69.5, 70.0, 70.5, 71.3. Anal. Calcd for $C_{17}H_{36}O_7$: C, 57.93; H, 10.29. Found: C, 57.13; H, 10.01.

*5,8,11,14,17,20,23-Heptaoxaheptacosane:Hexaethyleneglycol Dibutyl Ether (**15**).* Under N_2, 11.8 g (0.0573 mol) of triethyleneglycol monobutyl ether was added dropwise to a rapidly stirring suspension of 1.55 g (0.0646 mol) of NaH and 200 mL of THF in a 200 mL flask. After the addition was complete, 23.9 g (0.0664 mol) of **3** was added dropwise. The reaction mixture was allowed to stir for 24 h and filtered, and the volatiles were removed in vacuo. The crude product was distilled thrice (bp 163 °C/0.03 Torr) yielding 5.6 g (25%) of product as a yellow liquid. ^{1}H NMR δ 0.88 (t, 6H), 1.33 (m, 4H), 1.53 (m, 4H), 3.43 (t, 4H), 3.55 (m, 4H), 3.62 (m, 20H). ^{13}C NMR δ 13.08, 18.41, 30.89, 69.24, 69.73, 70.16. Anal. Calcd for $C_{20}H_{42}O_7$: C, 60.88; H, 10.73. Found: C, 60.10; H, 10.73.

Ba(hfa)$_2$·polyether Synthesis. *Typical Ba(hfa)$_2$·polyether Synthesis in Toluene (Method A).* Under N_2, 0.0063 mol of polyether was added to a stirring suspension of 0.0063 mol of Ba(hfa)$_2$ and 50 mL of heptane. The reaction mixture was stirred for 2 h, the volatiles were removed in vacuo, and the product was dried in vacuo overnight (10^{-2} Torr). The solid was then transferred to a sublimer (equipped with an ice-chilled water coldfinger), evacuated ($<10^{-4}$ Torr), and heated until sublimation began.

Typical Ba(hfa)$_2$·polyether Synthesis in Water (Method B). In a 1-L round-bottom flask fitted with an addition funnel, 14.9 g (0.0570 mol) of 99.999% Ba(NO$_3$)$_2$ and 1.00 equiv of the desired glyme were dissolved in 200 mL of distilled, deionized water. Simultaneously, 2.00 equiv of H(hfa) and 100 mL of DMF were placed in a 500 mL Erlenmeyer flask, and 2.00 equiv of *n*-PrNH$_2$ was *slowly* added (in 0.5 mL increments). The bright yellow *n*-PrNH$_3^+$hfa$^-$ solution was then transferred to the addition funnel and added dropwise to the Ba^{2+} solution at a rate of 1 drop/s. Following the addition, the reaction mixture was stirred for 1 h, and the solids were collected by suction filtration on a fritted glass funnel, washed twice with 50 mL of distilled deionized water, and then dried in vacuo. The products were then sublimed in vacuo (pressure $\leq 10^{-4}$ Torr; coldfinger cooled with recirculating water at 0 °C), or recrystallized from heptane for X-ray analysis, to yield the Ba(hfa)$_2$·polyether complexes as analytically pure, colorless crystalline materials.

*Ba(hfa)$_2$·triglyme·H$_2$O (**16**).* In a 500-mL round-bottom flask 4.6 g (0.017 mol) Ba(NO$_3$)$_2$ was dissolved in 4.7 g (0.026 mol) triglyme, 100 mL of DMF, and 10 mL of distilled H$_2$O. Simultaneously, a 500 mL Erlenmeyer flask was charged with 100 mL of DMF, 7.3 g (0.035 mol) of H(hfa), and 2.2 g (0.037 mol) of *n*-PrNH$_2$ (*added to the hfa/DMF with rapid stirring*). The *n*-PrNH$_3^+$hfa$^-$ solution was then transferred to the stirring Ba(NO$_3$)$_2$ solution, the reaction allowed to continue for 1 h and filtered, and the filtrate reduced to a yellow slurry in vacuo. The slurry was then poured into 100 mL of distilled H$_2$O, agitated, and filtered (this procedure is repeated thrice). The solids were air-dried overnight and sublimed (120 °C/0.05 Torr) yielding 6.11 g (47%) of colorless product. Mp 103−104 °C. ^{1}H NMR δ 1.94 (s, H$_2$O), 3.30 (s, 6H), 3.58 (m, 4H), 3.70 (m, 2H), 3.73 (s, 6H), 5.85 (s, 2H). ^{19}F NMR δ −77.19. ^{13}C NMR δ 58.7, 69.8, 70.0, 71.3, 87.5, 118.0 (q, 286.8 Hz), 175.3 (q, 31.8 Hz). Anal. Calcd for $C_{18}H_{22}O_9F_{12}Ba$: C, 28.88; H, 2.96. Found: C, 28.81; H, 2.85. MS (EI, *m*/*e*+) 897 amu (Ba$_2$hfa$_3$). IR (cm^{-1}, intensity) 3482 (w, br), 2949 (w, br), 1674 (s), 1531 (s), 1512 (s), 1472 (m), 1457 (w), 1351 (w), 1258 (s), 1207 (s), 1145 (s), 1137 (s), 1093 (s), 1068 (m), 949 (w), 867 (w), 845 (w), 791 (s), 759 (w), 662 (s), 577 (s), 525 (w).

*Ba(hfa)$_2$·triethyleneglycol Methylethyl Ether·H$_2$O (**17**).* In a 1-L round-bottom flask, 3.6 g (0.014 mol) of Ba(NO$_3$)$_2$ was dissolved in 2.5 g (0.013 mol) of triglyme, 300 mL of DMF, and 4 mL of distilled H$_2$O. Simultaneously, a 500 mL Erlenmeyer flask was charged with 300 mL of DMF, 5.0 g (0.024 mol) H(hfa), and 1.5 g (0.025 mol) of *n*-PrNH$_2$ (*added to the hfa/DMF with rapid stirring*). The *n*-PrNH$_3^+$hfa$^-$ solution was then transferred to the stirring Ba(NO$_3$)$_2$ solution and the reaction continued for 1 h, after which time the DMF was removed in vacuo. The remaining yellow slurry was poured into 100 mL of distilled H$_2$O, stirred, and filtered. The filtrate was extracted twice with 100 mL of diethyl ether, and the combined organics were dried over Na$_2$SO$_4$, filtered, and concentrated in vacuo. The resulting yellow oil was dissolved in boiling heptane, slowly cooled to −10 °C and allowed to stand undisturbed for crystallization (2 days). The resulting crystals, as well as the H$_2$O-insoluble precipitates, were combined and recrystallized from boiling heptane affording 3.74 g (41%) of colorless product. Mp 74−76 °C. ^{1}H NMR δ 1.14 (m, 3H), 1.93 (s, H$_2$O), 3.30 (s, 3H), 3.54 (m, 2H), 3.60 (m, 4H), 3.71 (m, 2H), 3.74 (s, 6H), 5.86 (s, 2H). ^{19}F NMR δ −77.41. ^{13}C NMR δ 14.0, 58.8, 67.3, 68.8, 69.8, 70.0, 70.1, 71.3, 87.4, 118.0 (q, 287.2 Hz), 175.3 (q, 31.9 Hz). Anal. Calcd for $C_{19}H_{24}O_9F_{12}Ba$: C, 29.96; H, 3.18. Found: C, 29.46; H, 2.91. MS (EI, *m*/*e*+) 897 amu (Ba$_2$hfa$_3$). IR (cm^{-1}, intensity) 3505 (w, br), 2948 (w, br), 2351 (w), 1672 (s), 1529 (s), 1514 (s), 1470 (m), 1459 (w), 1349 (w), 1256 (s), 1204 (s), 1143 (s), 1092 (s), 1066 (m), 943 (m), 862 (m), 791 (s), 758 (w), 737 (w), 661 (s), 578 (s), 525 (w).

*Ba(hfa)$_2$·triethyleneglycol Methyl 2-Methoxybutyl Ether (**18**, Methods A and B).* Yield 67% (*A*) and 63% (*B*). Mp 111−114 °C. ^{1}H NMR δ 1.14 (d, 3H), 1.80 (m, 2H), 3.15 (s, 3H), 3.31 (s, 3H), 3.47 (m, 2H), 3.56 (m, 4H), 3.57 (m, 4H), 3.64 (m, 6H),

3.72 (m, 2H), 3.90 (m, 1H), 5.83 (s, 2H). ^{13}C NMR δ 17.6, 34.9, 55.6, 58.6, 69.6, 69.8, 70.2, 70.5, 70.7, 70.8, 70.9, 78.0, 87.0, 118.2 (q, 330.2 Hz), 174.9 (q, 31.9 Hz). ^{19}F NMR δ −77.44 (s). Anal. Calcd for $C_{22}H_{28}O_9F_{12}Ba$: C, 32.92; H, 3.52. Found: C, 32.81; H, 3.47. MS (EI, *m/e*+) 801 amu. IR (cm^{-1}, intensity) 2942 (m), 1670 (s), 1527 (s), 1474 (m), 1350 (m), 1253 (s), 1203 (s), 1144 (s), 1095 (m), 1078 (m), 944 (w), 793 (m), 751 (w), 658 (s), 577 (m), 424 (w).

*Ba(hfa)$_2$·tetraethyleneglycol Dimethyl Ether (**19**, Method B).* Yield 63%. Mp 151−152 °C. ^{1}H NMR δ 3.34 (s, 6H), 3.45 (m, 4H), 3.56 (m, 4H), 3.73 (m, 4H), 3.80 (m, 4H), 5.82 (s, 2H). ^{13}C NMR δ 58.9, 69.9, 70.0, 70.5, 71.0, 86.9, 118.2 (q, 330.2 Hz), 174.9 (q, 31.9 Hz). ^{19}F NMR δ −77.14 (s). Anal. Calcd for $C_{20}H_{24}O_9F_{12}Ba$: C, 31.05; H, 3.13. Found: C, 31.19; H, 2.99. IR (cm^{-1}, intensity) 2930 (m), 2846 (m), 2363 (w), 1665 (s), 1526 (s), 1472 (m), 1454 (w), 1255 (s), 1202 (s), 1143 (s), 1088 (s), 1025 (w), 950 (m), 854 (w), 793 (m), 755 (w), 658 (m), 578 (m), 526 (w).

*Ba(hfa)$_2$·tetraethyleneglycol Dibutyl Ether (**20**, Method A).* Yield 46%. Mp 90−91 °C. ^{1}H NMR δ 0.84 (t, 6H), 1.21 (m, 4H), 1.51 (m, 4H), 3.49 (m, 8H), 3.58 (m, 4H), 3.74 (m, 8H), 5.81 (s, 2H). ^{13}C NMR δ 13.56, 18.75, 30.46, 60.73, 68.76, 70.40, 70.63, 71.61, 86.78, 118.16 (q, 287.63 Hz), 174.64 (q, 31.8 Hz). ^{19}F NMR δ −77.28 (s). Anal. Calcd for $C_{26}H_{36}O_9F_{12}$-Ba: C, 36.40; H, 4.23. Found: C, 36.57; H, 4.35. MS (EI, *m/e*+) 858 amu. IR (cm^{-1}, intensity) 2963 (m), 2878 (m), 1669 (s), 1528 (s), 1470 (m), 1348 (m), 1256 (s), 1190 (s), 1142 (s), 1078 (s), 943 (m), 791 (w), 760 (m), 737 (w), 660 (m), 577 (m), 525 (w).

*Ba(hfa)$_2$·tetraethyleneglycol Methylhexyl Ether (**21**, Methods A and B).* Yield 16% (*A*) and 51% (*B*). Mp 43−48 °C. ^{1}H NMR δ 0.83 (t, 3H), 1.19 (m, 6H), 1.54 (m, 2H), 3.34 (s, 3H), 3.47 (m, 6H), 3.56 (m, 4H), 3.75 (m, 8H), 5.81 (s, 2H). ^{13}C NMR δ 13.84, 22.46, 25.12, 28.36, 31.45, 58.61, 68.84, 69.70, 69.88, 70.11, 70.27, 70.59, 70.92, 72.10, 86.91, 118.16 (q, 288 Hz), 174.80 (q, 32 Hz). ^{19}F NMR δ −77.31 (s). Anal. Calcd for $BaC_{25}H_{34}O_9F_{12}$: C, 35.58; H, 4.06. Found: C, 35.71; H, 4.05. MS (EI, *m/e*+) 846 amu. IR (cm^{-1}, intensity) 2945 (m), 2868 (m), 1669 (s), 1532 (s), 1470 (m), 1360 (m), 1254 (s), 1194 (s), 1142 (s), 1084 (s), 947 (m), 860 (w), 791 (m), 764 (w), 660 (m), 577 (m), 525 (w).

*Ba(hfa)$_2$·pentaethyleneglycol (**22**, Method B).* Yield 44%. Mp 169−173 °C. ^{1}H NMR δ 3.1 (v br, 2H), 3.62 (m, 8H), 3.70 (s, 4H), 3.73 (m, 8H), 5.82 (s, 2H). ^{19}F NMR δ −77.21. Anal. Calcd for $C_{20}H_{24}O_{10}F_{12}Ba$: C, 30.42; H, 2.90. Found: C, 30.27; H, 3.10. MS (EI, *m/e*+) 791 amu. IR (cm^{-1}, intensity) 3465 (br, m), 3119 (br, w), 2938 (sh, m), 2356 (br, w), 1669 (s), 1532 (s), 1510 (m), 1469 (m), 1391 (w), 1358 (w), 1305 (m), 1256 (s), 1198 (s), 1145 (s), 1108 (m), 1086 (s), 950 (m), 891 (w), 823 (w), 790 (m), 760 (w), 660 (s), 576 (m), 525 (w), 445 (w).

*Ba(hfa)$_2$·pentaethyleneglycol Methylethyl Ether (**23**, Method B).* Yield 70%. Mp 109−111 °C. ^{1}H NMR δ 1.15 (m, 3H), 1.48 (br, 2H), 3.27 (s, 3H), 3.42 (m, 2H), 3.56 (m, 12H), 3.70 (m, 8H), 5.77 (s, 2H). ^{13}C NMR δ 13.6, 58.9, 66.1, 68.5, 69.2, 69.6, 69.7, 69.9, 70.0, 70.2, 70.5, 72.2, 86.2 (q, 7.3 Hz), 118.3 (q, 288 Hz), 174.2 (q, 31 Hz). ^{19}F NMR δ −77.29. Anal. Calcd for $C_{23}H_{30}O_{10}F_{12}Ba$: C, 33.21; H, 3.65. Found: C, 32.97; H, 3.56. MS (EI, *m/e*+) 831 amu. IR (cm^{-1}, intensity) 2941 (m), 1670 (s), 1532 (s), 1475 (w), 1358 (w), 1255 (s), 1197 (s), 1145 (s), 1090 (s), 953 (m), 857 (w), 790 (m), 759 (w), 660 (s), 576 (m).

*Ba(hfa)$_2$·pentaethyleneglycol Methylbutyl Ether (**24**, Method B).* Yield 83%. Mp 75−76 °C. ^{1}H NMR δ 0.85 (t, 3H), 1.19 (m, 2H), 1.48 (m, 2H), 3.27 (s, 3H), 3.42 (t, 2H), 3.57 (m, 12H), 3.70 (m, 8H), 5.77 (s, 2H). ^{13}C NMR δ 13.75, 18.73, 30.05, 58.91, 68.96, 69.16, 69.65, 69.75, 69.89, 70.00, 70.23, 70.43, 70.81, 72.13, 86.24, 118.28 (q, 288 Hz), 174.21 (q, 31 Hz). ^{19}F NMR δ −77.18 (s). Anal. Calcd for $C_{25}H_{34}O_{10}F_{12}Ba$: C, 34.92; H, 3.99. Found: C, 35.39; H, 3.98. MS (EI, *m/e*+) 859 amu. IR (cm^{-1}, intensity) 2934 (m), 2888 (m), 1670 (s), 1532 (s), 1472 (m), 1352 (m), 1256 (s), 1192 (s), 1144 (s), 1094 (s), 951 (m), 856 (w), 789 (m), 754 (w), 660 (m), 577 (m), 525 (w).

*Ba(hfa)$_2$·pentaethyleneglycol Methylhexyl Ether (**25**, Methods A and B).* Yield 65% (*A*) and 40% (*B*). Mp 68−73 °C. ^{1}H NMR δ 0.84 (t, 3H), 1.21 (m, 6H), 1.50 (m, 2H), 3.28 (s, 3H), 3.42 (t, 2H), 3.60 (m, 12H), 3.73 (m, 8H), 5.77 (s, 2H). ^{13}C NMR δ 13.89, 22.55, 25.19, 27.98, 31.63, 58.92, 68.92, 69.15, 69.61, 69.74, 69.88, 70.00, 70.24, 70.45, 71.07, 72.13, 86.24, 118.27 (q, 288 Hz), 174.20 (q, 30.75 Hz). ^{19}F NMR δ −77.18 (s). Anal. Calcd for $C_{27}H_{38}O_{10}F_{12}Ba$: C, 36.52; H, 4.31. Found: C, 36.49; H, 4.36. MS (EI, *m/e*+) 888 amu. IR (cm^{-1}, intensity) 2940 (m), 2878 (m), 1670 (s), 1532 (s), 1470 (m), 1352 (m), 1256 (s), 1196 (s), 1142 (s), 1086 (s), 957 (m), 856 (w), 789 (m), 752 (w), 650 (m), 575 (m), 525 (w).

*Ba(hfa)$_2$·pentaethyleneglycol Ethylbutyl Ether (**26**, Methods A and B).* Yield 12% (A) and 79% (B). Mp 71−72 °C. ^{1}H NMR δ 0.85 (t, 3H), 1.10 (t, 3H), 1.19 (m, 2H), 1.48 (m, 2H), 3.43 (t, 2H), 3.54 (t, 2H), 3.58 (m, 8H), 3.63 (s, 4H), 3.69 (m, 8H), 5.77 (s, 2H). ^{13}C NMR δ 13.71, 18.73, 18.99, 30.21, 66.05, 68.13, 68.87, 69.71, 69.90, 70.09, 70.44, 70.86, 86.26, 118.27 (q, 288.1 Hz), 174.20 (q, 31.43 Hz). ^{19}F NMR δ −77.34 (s). Anal. Calcd for $C_{26}H_{36}O_{10}F_{12}Ba$: C, 35.74; H, 4.15. Found: C, 36.79; H, 4.39. MS (EI, *m/e*+) 874 amu. IR (cm^{-1}, intensity) 2936 (m), 2880 (m), 1670 (s), 1532 (s), 1472 (m), 1352 (m), 1254 (s), 1192 (s), 1144 (s), 1092 (s), 953 (m), 851 (w), 791 (m), 752 (w), 660 (m), 575 (m), 525 (w).

*Ba(hfa)$_2$·pentaethyleneglycol Butylhexyl Ether (**27**, Method A).* Yield 98%. Mp 34−36 °C. ^{1}H NMR δ 0.86 (t, 6H), 1.20 (m, 8H), 1.47 (m, 4H), 3.42 (m, 4H), 3.63 (m, 20H), 5.77 (s, 2H). ^{13}C NMR δ 13.75, 18.96, 30.89, 69.68, 69.77, 69.83, 70.04, 70.13, 70.29, 70.93, 86.61, 118.21 (q, 287.85 Hz), 174.40 (q, 29.03 Hz). ^{19}F NMR δ −77.10 (s). Anal. Calcd for $C_{30}H_{44}O_{10}F_{12}Ba$: C, 38.75; H, 4.77. Found: C, 39.45; H, 4.60. MS (EI, *m/e*+) 929 amu. IR (cm^{-1}, intensity) 2936 (m), 2876 (m), 1669 (s), 1534 (s), 1468 (m), 1381 (m), 1252 (s), 1192 (s), 1136 (s), 1090 (s), 955 (m), 847 (w), 791 (m), 754 (w), 660 (m), 577 (m), 525 (w).

*Ba(hfa)$_2$·hexaethyleneglycol (**28**, Method B).* Yield 15%. Mp 109−112 °C. ^{1}H NMR δ 3.65 (s, 20H), 3.73 (m, 4H), 5.01 (s, 2H), 5.78 (s, 2H). ^{13}C NMR δ 60.4, 69.5, 69.9, 70.2, 70.5, 72.2, 86.5, 118.2 (q, 287.7 Hz), 174.60 (q, 31.6 Hz). ^{19}F NMR δ −77.17 (s). Anal. Calcd for $C_{22}H_{28}O_{11}F_{12}Ba$: C, 31.69; H, 3.38. Found: C, 31.71; H, 3.34. IR (cm^{-1}, intensity) 3300 (br, m), 2933 (m), 2882 (w), 1669 (s), 1532 (s), 1472 (w), 1356 (w), 1256 (s), 1192 (s), 1146 (s), 1082 (s), 956 (m), 837 (w), 791 (m), 758 (w), 660 (s), 578 (m), 525 (w).

*Ba(hfa)$_2$·hexaethyleneglycol Methylbutyl Ether (**29**, Method B).* Yield 50%. Mp 52−54 °C. ^{1}H NMR δ 0.82 (m, 3H), 1.20 (m, 2H), 1.43 (m, 2H), 3.20 (s, 3H), 3.31 (m, 2H), 3.42 (m, 2H), 3.46 (m, 2H), 3.53 (s, 14H), 3.60 (s, 8H), 5.73 (s, 2H). ^{13}C NMR δ 13.7, 18.9, 30.8, 58.6 68.1, 68.3, 68.5, 68.9, 69.0, 69.2, 69.26, 69.35, 69.4, 69.9, 70.8, 71.2, 86.0, 118.1 (q, 288.6 Hz), 175.2 (q, 30.9 Hz). ^{19}F NMR δ −76.62 (s). Anal. Calcd for $C_{27}H_{38}O_{11}F_{12}Ba$: C, 35.88; H, 4.21. Found: C, 36.21; H, 4.46. IR (cm^{-1}, intensity) 1681 (s), 1555 (s), 1474 (m), 1460 (w), 1374 (w), 1355 (m), 1261 (s), 1204 (s), 1145 (s), 1070 (s), 1030 (w), 1015 (w), 985 (w), 942 (s), 911 (w), 897 (w), 864 (w), 789 (s), 751 (m), 736 (m), 714 (w), 660 (s), 621 (w), 575 (s), 542 (w), 525 (w), 446 (w).

*Ba(hfa)$_2$·hexaethyleneglycol Dibutyl Ether (**30**, Method A).* Yield 98%. Mp −64 °C (determined using a dry ice/acetone cooling bath). ^{1}H NMR δ 0.85 (m, 6H), 1.24 (m, 4H), 1.46 (t, 4H), 3.38 (m, 4H), 3.52 (m, 4H), 3.67 (m, 20H), 5.79 (s, 2H). ^{13}C NMR δ 13.56, 18.75, 30.46, 60.73, 68.76, 70.40, 70.63, 71.61, 86.78, 118.16 (q, 287.63 Hz), 174.64 (q, 31.8 Hz). ^{19}F NMR δ −77.10 (s). Anal. Calcd for $C_{30}H_{44}O_{11}F_{12}Ba$: C, 38.09; H, 4.69. Found: C, 37.18; H, 4.54. MS (EI, *m/e*+) 947 amu. IR (cm^{-1}, intensity) 2947 (m), 2870 (m), 1670 (s), 1530 (s), 1468 (m), 1354 (m), 1254 (s), 1192 (s), 1142 (s), 1096 (s), 953 (m), 789 (m), 756 (w), 750 (w), 660 (m), 577m (s), 525 (w).

Results and Discussion

Precursor Synthesis and Characterization. Structural modification of the polyether ligands was accomplished using a modified Williamson ether synthetic approach paralleling the procedure of Dale and Kristianson (Scheme 1).[21] This route employs the nucleophilic attack of a polyether alkoxide (generated in situ) on a tosylated oligoethyleneglycol monoalkyl in

(21) Dale, J.; Kristianson, P. O. *Acta Chem. Scand.* **1972**, *26*, 1471.

Scheme 1. Modified Williamson Ether Synthesis Employed for the Polyether Ligand Synthesis

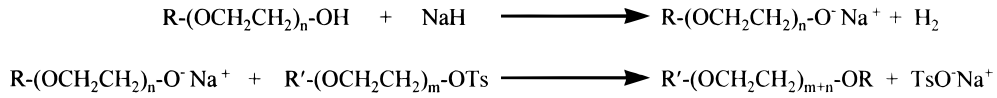

R′ (tosylate)	m	compound
CH_3	3	**2**
C_4H_9	3	**3**
C_6H_{13}	2	**4**

R′, R (product)	m+n	compound
CH_3, $C_5H_{11}O$	3	**6**
C_4H_9, C_4H_9	4	**7**
C_6H_{13}, CH_3	4	**8**
CH_3, C_2H_5	5	**9**
CH_3, C_4H_9	5	**10**
C_6H_{13}, CH_3	5	**11**
C_4H_9, C_2H_5	5	**12**
C_4H_9, C_6H_{13}	5	**13**
C_4H_9, CH_3	6	**14**
C_4H_9, C_4H_9	6	**15**

Scheme 2. Anhydrous and Aqueous Synthetic Approaches to Ba(hfa)$_2$·polyether MOCVD Precursors

Method A (anhydrous)

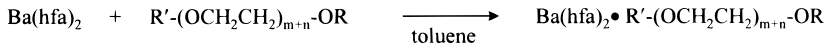

Method B (aqueous)

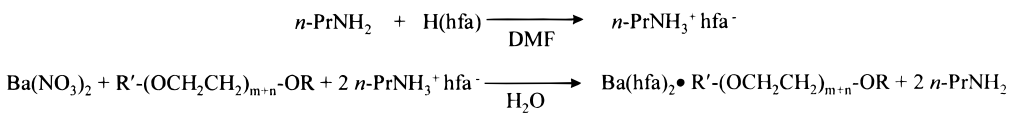

R′, R (glyme)	m+n	product
CH_3, CH_3	3	**16**
CH_3, C_2H_5	3	**17**
CH_3, $C_5H_{11}O$	3	**18**
CH_3, CH_3	4	**19**
C_4H_9, C_4H_9	4	**20**
C_6H_{13}, CH_3	4	**21**

R′, R (glyme)	m+n	product
OH, OH	5	**22**
CH_3, C_2H_5	5	**23**
CH_3, C_4H_9	5	**24**
C_6H_{13}, CH_3	5	**25**
C_4H_9, C_2H_5	5	**26**
C_4H_9, C_6H_{13}	5	**27**
OH, OH	6	**28**
C_4H_9, CH_3	6	**29**
C_4H_9, C_4H_9	6	**30**

THF. The advantage of this approach is that the final products have boiling points significantly different from either the tosylate or hydrolyzed alkoxide, greatly simplifying purification. Furthermore, this route is amenable to large scale synthesis (moles), which is particularly attractive given the low cost and abundant supply of starting materials.

Two different methods (anhydrous and aqueous) were employed for the Ba(hfa)$_2$·polyether syntheses. In method A (Scheme 2), the desired polyether is added to a stirring suspension of Ba(hfa)$_2$ in toluene, and the product subsequently purified.[22] The drawbacks of this route are the cost of commercial Ba(hfa)$_2$, low yields, and the limited metals purity available. The second approach (method B, Scheme 2), developed in this laboratory,[23] uses the aqueous reaction of $Ba(NO_3)_2$ (available in 99.999% metal purity) and polyether, with *n*-$PrNH_3^+hfa^-$ and exploits the complete aqueous insolubility of the crude metal complexes as an initial purification step. The recovered solids can then be filtered, dried, and sublimed to yield the desired Ba(hfa)$_2$·polyethers in high yield and analytical purity.

The general class of Ba(hfa)$_2$·polyether complexes are nonhygroscopic, air-stable, colorless crystalline solids that are stable to repeated thermal cycling. They are readily soluble in polar organic media (e.g., $CHCl_3$, acetone, and benzene) but have only modest solubility in either linear or cyclic alkanes. The ^1H and ^{19}F NMR spectroscopic data for these complexes are as expected and are in accord with the proposed molecular structures assuming stereochemically nonrigid coordination spheres.[24] The mass and infrared spectra warrant additional comments, however. The mass spectra of the Ba(hfa)$_2$·polyether complexes (polyether ≥ tetraglyme) give no indication of gas-phase oligomers, directly contrasting reported results for Ba(β-diketonate)$_2$[25] and Ba(dpm)$_2$·polyether[11,26] complexes. The exclusively monomeric nature of the Ba(hfa)$_2$·polyether complexes is presumably due to the strong ligation of the Ba^{2+} center by the hfa^- and glyme ligands, thus maintaining coordinative saturation in the gas phase. Similarly, infrared results (where crystallography was considered redundant) fully support the monomeric molecular formulations in the crystal lattice. Particularly noteworthy is

(22) Timmer, K; Meinema, H. A. *Inorg. Chim. Acta* **1991**, *187*, 99.
(23) Schulz, D. L.; Neumayer, D. A.; Marks, T. J. *Inorg. Synth.* **1997**, *31*, 1.

(24) (a) Evans, D. F.; Jakubovic, D. A. *J. Chem. Soc., Chem. Commun.* **1988**, 1612. (b) Douglas, B. E.; McDaniel, D. H.; Alexander, J. J. *Concepts and Models of Inorganic Chemistry*; John Wiley & Sons: New York, 1983; p 325. (c) Drew, M. G. B. *Coord. Chem. Rev.* **1977**, *24*, 179. (d) Muetterties, E. L. *Acc. Chem. Res* **1970**, *3*, 266.
(25) (a) Ryu, H. K.; Han, J. H.; Moon, A. H. *Mater. Res. Soc. Symp. Proc.* **1996**, *415*, 161. (b) Schwarberg, J. E.; Sievers, R. B.; Moshier, R. W. *Anal. Chem.* **1970**, *42*, 1828.
(26) Luten, H. A.; Otway, D. J.; Rees, W. S. *Mater. Res. Soc. Symp. Proc.* **1996**, *415*, 99.

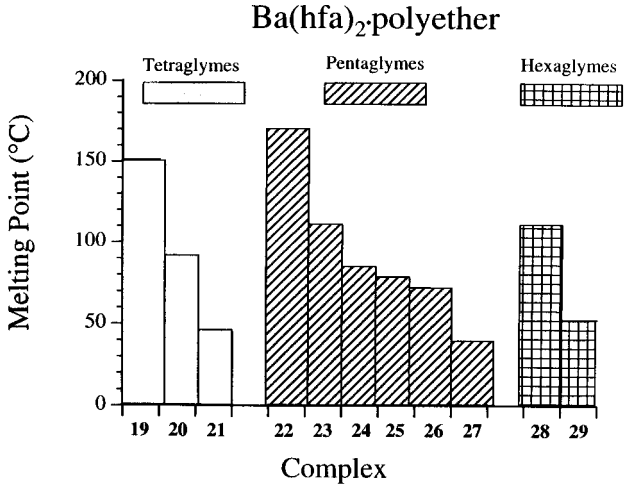

Figure 2. Melting point tunability of the new Ba(hfa)·-polyether complexes.

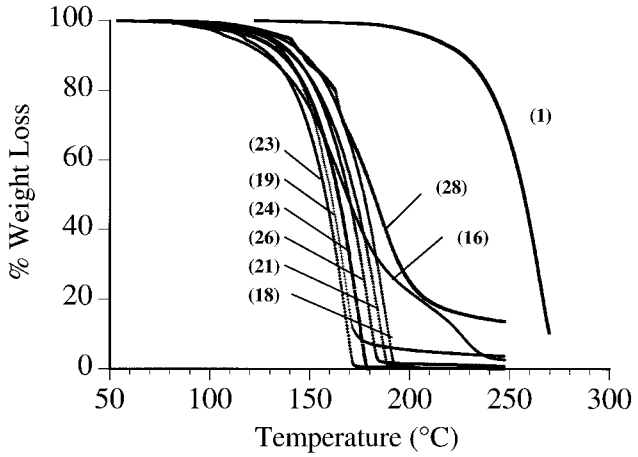

Figure 3. Thermogravimetric data for precursors **1**, **16**, **18**, **19**, **21**, **23**, **24**, **26**, and **28** recorded at a ramp rate of 1.5 °C/min and at 5.0 Torr of N_2.

the simplicity[10a] of the ν(C═O) (1700−1600 cm^{-1}) and ν(C═C) (1600−1500 cm^{-1}) regions when compared to the reported data for crystallographically characterized β-diketonate oligomers.[2a,11a]

Volatility Studies. A major impetus for this work was the development of lower melting and more volatile Ba^{2+} MOCVD sources than **19**. The approach focused on modifying the polyether appendage, in both the number of $-OCH_2CH_2-$ linkages and end groups, to explore the impact of subtle structural changes on melting and volatility properties. In Figure 2, the melting points and structure−melting point trends for the new Ba(hfa)$_2$·polyether complexes are summarized, and two distinct conclusions can be drawn. First, there is little effect on the melting point when proceeding from tetraglyme to pentaglyme; however, upon addition of an additional $-OCH_2CH_2-$ unit, the high end of the melting point range is significantly depressed. This result can be best explained using known Ba(hfa)$_2$·-hexaglyme structural studies, which indicate the Ba^{2+} ion is fully saturated with 10 O atoms and that one of the terminal ether linkages extends untethered in the crystal lattice.[10e,14] This inherent molecular dissymmetry undoubtedly lowers the lattice stabilization energy and hence lowers the melting point. Although quantifying this structure−melting point relationship is difficult given the delicate balance of entropic and enthalpic effects, similar strategies to achieve structure−melting point tunability have been reported for organic poly(ethylene glycol) inclusion compounds.[27] The second striking feature of the present results is the complete melting point tunability within a given family. As expected, the melting point is inversely proportional to increasing steric bulk at the glyme terminus, with unsymmetrical substituents adding even greater flexibility and tunability to the design possibilities. Although we have not explored every conceivable substitution pattern, the 150 °C melting point range for the pentaglyme complexes explicitly demonstrates the potential of synthetic chemistry in the molecular structure properties engineering of new MOCVD precursors.

Equally important to developing suitable alkaline earth MOCVD precursors is the ability to quantify (and control) precursor volatility under conditions approaching those used for film growth.[2h,28] Accurately and appropriately characterizing the volatilities of CVD precursors has been problematic, and for the present types of precursors and growth reactors, precursor transport is likely to be diffusion-limited (operational vapor pressures never attain the equilibrium vapor pressures) and film growth is likely to be mass-transport limited.[15b] Thus, we recently developed a convenient method, based on reduced pressure thermogravimetric analysis (TGA), that allows the determination of precursor sublimation rate under near-CVD conditions.[15] In this manner, the working precursor temperature range (±10 °C) for any desired film stoichiometry can be established *before* introduction into the reactor system, and the relative transport characteristics of different precursors can be meaningfully compared. This information not only aids in designing optimum precursors but greatly constrains the parameter space (precursor reservoir temperature and pressure) that must be explored for successful film growth using every new precursor.

Figure 3 shows the raw TGA-derived weight loss data under 5.00 Torr (±0.05) N_2 for the most volatile of the present glyme complexes compared to a commercial sample of Ba(dpm)$_2$. It is immediately apparent that the Ba(hfa)$_2$·glyme complexes are far more volatile and sublime without residue (negligible decomposition), whereas the Ba(dpm)$_2$ samples are far less volatile and *do not* sublime completely. The thermal behavior of the latter complex indicates substantial decomposition and/or further solid-state oligomerization and is a serious impediment to maintaining a constant precursor vapor pressure as well as controlling product film stoichiometry.[28a]

Translation of raw TGA weight loss data into useful volatility information for CVD precursors has been a formidable challenge.[15a,29] It requires an inherent knowledge of the volatilization process, an understanding of film growth/reactor behavior, and a method for establishing some type of volatility relationship between current and potential precursors. Figure 4 shows

(27) (a) Suehiro, K.; Kuramori, M. *J. Macromol. Sci. Phys.* **1994**, *B33*, 1. (b) Schmidt, G.; Enkelmann, V.; Westphal, U.; Droscher, M.; Wegner, G. *Colloid Polym. Sci.* **1985**, *263*, 120. (c) Suehiro, K.; Urabe, A.; Yoshitake, Y.; Nagano, Y. *Makromol. Chem.* **1984**, *185*, 2467.

(28) (a) Rappoli, B. J.; DeSisto, W. J. *Appl. Phys. Lett.* **1996**, *68*, 2726. (b) Schmader, F.; Huber, R.; Oetzmann, H.; Wahl, G. *Appl. Surf. Sci.* **1990**, *46*, 53.

(29) (a) Chou, K. S.; Tsai, G. J. *Thermochim. Acta* **1994**, *240*, 129. (b) Chou, K. S.; Hwang, M. J.; Tsai, G. J. *Thermochim. Acta* **1994**, *233*, 141.

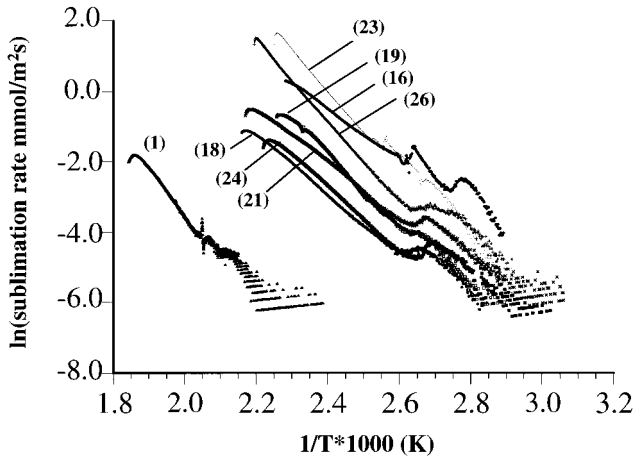

Figure 4. Arrhenius plots comparing the molecular volatility of precursors **1**, **16**, **18**, **19**, **21**, **23**, **24**, and **26** at a ramp rate of 1.5 °C/min and at 5.0 Torr of N_2.

volatilization Arrhenius plots, corrected for diffusion distance,[15a] of the most volatile Ba(hfa)$_2$·glyme complexes identified in this study. It is readily apparent that *all* of these compounds are significantly more efficient (and stable) sources of gas-phase Ba than Ba(dpm)$_2$. In addition, the most promising precursor identified thus far, Ba(hfa)$_2$·pentaethyleneglycol methylethyl ether (**23**), has a melting point ~45 °C lower than the commonly used Ba(hfa)$_2$·tetraethyleneglycol dimethyl ether (**19**) and significantly greater volatility. This molecule represents an example of successful structural engineering of a liquid Ba source, and its superior volatility doubtless reflects lowered lattice stabilization energy (through unsymmetrical etheric end groups) without increased intermolecular interactions (see structural discussion below). As a cautionary note, although several of the glyme complexes prepared in this study have lower melting points than **19**, their molecular sublimation rate (volatility) is not higher.

Molecular Structure Studies. The single-crystal X-ray structures of Ba(hfa)$_2$·triglyme·H_2O (**16**) and Ba(hfa)$_2$·pentaethyleneglycol methylethyl ether (**23**) expectedly reveal that polyether and hfa ligation is only through the oxygen atoms. The molecular structures of complexes **16** and **23** are similar to those of other known M^{2+}(β-diketonate)$_2$·polyether structures (and also a variety of glyme−M^{2+} main-group complexes[30]) with the glyme residing in a meridional plane and the two hfa ligands, above and below this plane, with the hfa planes in a pseudoorthogonal relationship.[2h,10d,e,11a,14,26,31] Metrical parameters are compiled in Table 2. The Ba−O(diketonate) bond distances range from 2.698(3) to 2.760(3) Å and from 2.763(3) to 2.819(3) Å in **16** and **23**, respectively, similar to other structurally characterized Ba(hfa)$_2$·polyether complexes.[2h,10d,e,14,31] The Ba−O(polyether) bond distances range from 2.809(3) to 2.847(3) Å and from 2.813(3) to 2.887(3) Å in **16** and **23**, respectively, again being quite similar to other structurally characterized Ba(hfa)$_2$·polyether complexes.[2h,10d,e,14,31]

The molecular structure of **16** consists of a mononuclear complex in which two hfa ligands, a triglyme, and an H_2O molecule are coordinated through the

Table 2. Selected Bond Lengths (Å) and Angles (deg) for Ba(hfa)$_2$·triglyme·H_2O (16) and Ba(hfa)$_2$·methylethylpentaglyme (23)[a]

bond lengths (Å)	**16**	**23**
Ba−O1	2.760(3)	2.842(3)
Ba−O2	2.723(3)	2.887(3)
Ba−O3	2.698(3)	2.813(3)
Ba−O4	2.757(3)	2.827(3)
Ba−O5	2.843(3)	2.865(3)
Ba−O6	2.843(3)	2.845(3)
Ba−O7	2.809(3)	2.806(3)
Ba−O8	2.847(3)	2.775(3)
Ba−O9	2.760(3)	2.763(3)
Ba−O10	NA	2.819(3)

bond angles (deg)	**16**	bond angles (deg)	**23**
O1−Ba−O2	63.94(8)	O4−Ba−O1	156.43(10)
O1−Ba−O3	121.97(9)	O4−Ba−O2	118.9(1)
O1−Ba−O4	80.55(8)	O4−Ba−O3	61.7(1)
O1−Ba−O5	65.14(9)	O4−Ba−O5	60.1(1)
O1−Ba−O6	111.22(8)	O4−Ba−O6	117.6(1)
O1−Ba−O7	145.05(9)	O4−Ba−O7	73.3(1)
O1−Ba−O8	139.7(1)	O4−Ba−O8	81.77(9)
O1−Ba−O9	78.96(9)	O4−Ba−O9	122.75(10)
		O4−Ba−O10	65.03(9)

[a] The reported angles for **16** are for the capping atom, O1; those given for **23** are for the capping atom, O4.

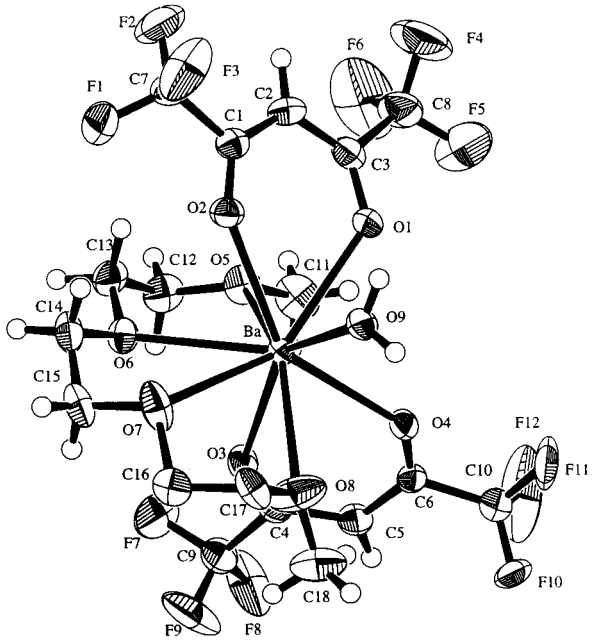

Figure 5. Perspective view of complex **16** illustrating the atomic numbering scheme. Thermal ellipsoids are drawn at 50% probability and H atoms have been omitted for clarity.

respective oxygen atoms, affording a Ba^{2+} coordination number of 9 (Figure 5). The hfa ligands defined by O1−O2−C1−C2−C3−C7−C8 and O3−O4−C4−C5−C6−C9−C10 are planar to within 0.0377 and 0.0431 Å, respectively. The Ba^{2+} ion is displaced from the O1−O2−C1−C2−C3−C7−C8 and O3−O4−C4−C5−C6−C9−C10 planes by 0.8532 and −0.0599 Å, respectively, and the O1−Ba−O2 and O3−Ba−O4 equilateral planes are tilted from the O1−O2−C1−C2−C3−C7−C8 and O3−O4−C4−C5−C6−C9−C10 planes by 21.7° and 15.7°, respectively. The dihedral angle between the O1−Ba−O2 and O3−Ba−O4 planes is 46.6°, 27.3° larger than in the 9-coordinate complex **19**.[2h]

The four coordinated ether oxygen atoms of **16** define a meridional plane that is planar to within 0.216 Å with a Ba displacement of −0.8635 Å from the mean-square plane. The dihedral angles between the meridional

(30) Rogers, R. D.; Bond, A. H.; Roden, D. M. *Inorg. Chem.* **1996**, *35*, 6964 and references therein.
(31) Motevalli, M.; O'Brien, P.; Watson, I. M. *Acta Crystallogr.* **1996**, *C52*, 3028.

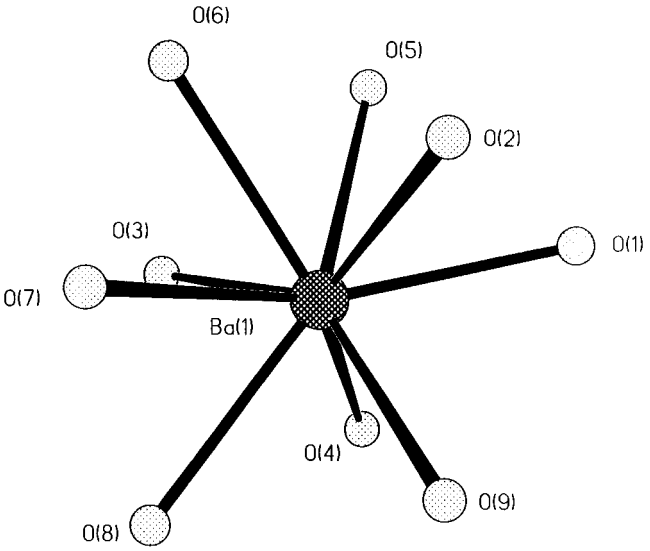

Figure 6. Immediate Ba^{2+} coordination geometry of complex **16** illustrating the distorted tricapped triangular prismatic geometry.

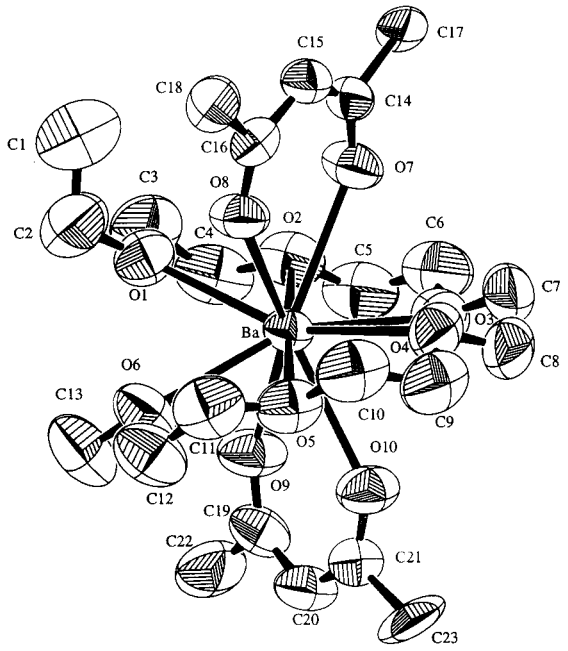

Figure 7. Perspective view of complex **23** illustrating the atomic numbering scheme. Thermal ellipsoids are drawn at 50% probability with H and F atoms omitted for clarity.

triglyme oxygen atom mean-square plane and the O1−Ba−O2 and O3−Ba−O4 planes are 58.4° and 96.5°, respectively. The coordinated O atom (triglyme and H_2O) meridional wrapping mode can best be described by a regular hexagon, with an O atom at each vertex (one is unoccupied in **16**) and Ba^{2+} at the center. The sequence of triglyme torsional angles in **16** is anti−gauche−anti, ag±a, with the signs of the gauche angles strictly alternating.[32] The result is a zigzag polyether configuration resulting in the observed wrapping mode coordination, typical of such complexes. The bound H_2O lies at a "virtual" triglyme site (i.e., it is not symmetrically bound in the meridional coordination void left by the tetradentate glyme), on the same side of the O1−Ba−O2 hfa ligand, with short O9−O1 (2.799 Å), O9−O4 (2.909 Å), and O9−F11 (3.13 Å) intermolecular distances suggestive of hydrogen bonding between two inversion related molecules.

The immediate coordination geometry about the Ba^{2+} center in complex **16** is best described as a distorted tricapped trigonal prism (Figure 6).[33] The trigonal prism vertexes are defined by O2 (hfa A), O5 (triglyme), and O6 (triglyme), and O4 (hfa B), O8 (triglyme), and O9 (water) atoms, with the capping atoms being O1 (hfa A), O3 (hfa B), and O7 (triglyme). The equilateral triangular planes defined by the vertexes and capping atoms are tilted with respect to each other, resulting in the distortion from an ideal tricapped trigonal prism. The dihedral angles between the plane defined by the capping atoms and Ba and the plane defined by the vertexes: O2, O5, O6 and O4, O8, O9 are 17.8° and 8.8°, respectively. The dihedral angle between two vertex planes is 23.3°. In a nondistorted tricapped trigonal prism the corresponding planes would be parallel, with a 0.0° dihedral angle between them. The distorted trigonal prismatic geometry is distinguished from the monocapped square antiprism by the O1−Ba−O8 angle of 139° and the O1−Ba−O3 angle of 122°. The corresponding angles in an ideal tricapped trigonal prism would be 135° and 120°, respectively, and in a monocapped square antiprism both angles are 127°.[33]

The molecular structure of $Ba(hfa)_2$·pentaethyleneglycol methylethyl ether (**23**) consists of a mononuclear complex in which the two hfa ligands and pentaethyleneglycol methylethyl ether are coordinated through their respective oxygen atoms, yielding a Ba^{2+} coordination number of 10 (Figure 7). As can be seen, the polyether terminal alkyl groups pack closely to the Ba^{2+} center, minimizing the possibility of intermolecular interactions, while their inherent dissymmetry/lipophilicity depresses the melting point.[27] The hfa ligands defined by C14−C15−O7−C16−C17−O8−C18 and C19−C20−O9−C21−C22−O10−C23 are planar to within 0.0394 and 0.0435 Å, respectively. The Ba^{2+} ion is displaced from the hfa C14−C15−O7−C16−C17−O8−C18 and C19−C20−O9−C21−C22−O10−C23 ligand planes by 0.0956 and 0.547 Å, respectively, and the O7−Ba−O8 and O9−Ba−O10 equilateral planes are tilted from the C14−C15−O7−C16−C17−O8−C18 and C19−C20−O9−C21−C22−O10−C23 planes by 12.3° and 23.0°, respectively. The dihedral angle between the O7−Ba−O8 and O9−Ba−O10 planes is 98.5°, comparable to the corresponding angle in similar 10-coordinate $Ba(hfa)_2$·polyether structures.[10e,14,31]

The coordinated ether oxygen atoms in complex **23** form a meridional plane that is planar to within 0.3915 Å with a Ba displacement of −0.0103 Å from the mean-square plane. The dihedral angles between the meridional pentaglyme plane and the O7−Ba−O8 and O9−Ba−O10 planes, which are almost normal, are 87.05° and 87.56°, respectively. The coordinated O atom meridional wrapping mode can be described by a regular hexagon, with an O atom at each vertex and Ba^{2+} at the center. The sequence of glyme torsional angles in **23** is again ag±a, with the signs of the gauche angles strictly alternating.[32]

The immediate coordination geometry about the Ba^{2+} center in **23** is best described as a slightly distorted tetradecahedron (cis-bicapped cube).[33] Figure 8 shows this coordination environment, with the two capping

(32) (a) Goldberg, I. In *Crown Ethers and Analogues*; Patai, S., Rappoport, Z., Eds.; John Wiley & Sons: Avon, 1989; pp 399−476. (b) Dale, J. *Isr. J. Chem.* **1980**, *20*, 3.

(33) (a) Favas, M. C.; Kepert, D. L. *Prog. Inorg. Chem.* **1981**, *28*, 309. (b) Robertson, B. E. *Inorg. Chem.* **1977**, *16*, 2735.

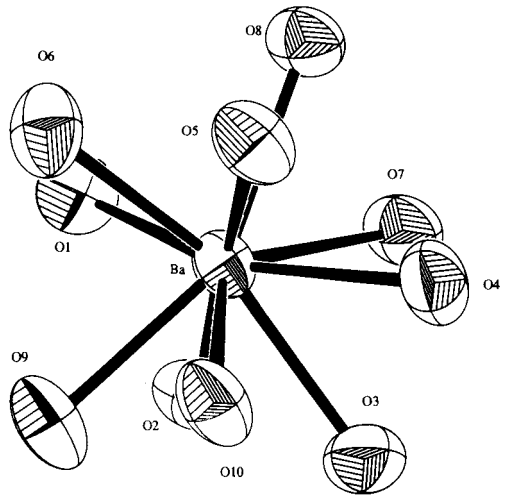

Figure 8. Immediate Ba^{2+} coordination geometry of complex **23** illustrating the slightly distorted tetradecahedral geometry.

oxygen atoms represented by O1 (pentaglyme) and O4 (pentaglyme). The planes defined by O1−O4−O6−O7 and O2−O5−O8−O10 are planar to within 0.6665 and 0.1238 Å with Ba displacements of 0.2771 and −0.1537 Å, respectively. The dihedral angle between these two planes is 89.5°, very close to the expected value of 90.0°. The large χ^2 value for the O1−O4−O6−O7 plane is probably attributable to steric repulsion between the terminal alkyl groups on O1 and O6, resulting in a terminal alkyl group "cis" conformation (the CH_3 and C_2H_5 each point toward an orthogonal hfa ligand).[31]

Implementation in MOCVD Thin Film Growth. To demonstrate the utility and efficiency of the new liquid Ba precursors, the growth of $BaTiO_3$ thin films was undertaken. To best match the high flux of the Ba precursor **23** through the reactor, $Ti(OC_2H_5)_4$ was employed as the Ti source. The in situ grown $BaTiO_3$ thin films are found to be epitaxial, with preferred growth along [100]. Repeated thermal cycling of **23** resulted in a slight yellow discoloration, but the complex retained a sharp melting point throughout the depositions.

The as-despoited $BaTiO_3$ films are transparent (with color fringes) and appear to be smooth and reflective. The XRD Θ−2Θ scans display only the (*h*00) reflections, indicative of exclusive *a*-axis orientation (Figure 9a).[34] The ω-rocking data obtained using the $BaTiO_3$ (200) reflection displays a relatively narrow full width at half-maximum of 0.55°, versus a value of 0.10° for the single-crystal $LaAlO_3$ (110) substrate reflection. In-plane epitaxy (*b*−*c* registry) is supported by the XRD ϕ scans of the $BaTiO_3$ {220} planes, with the requisite 4-fold symmetry at 90° intervals being observed (Figure 9b).

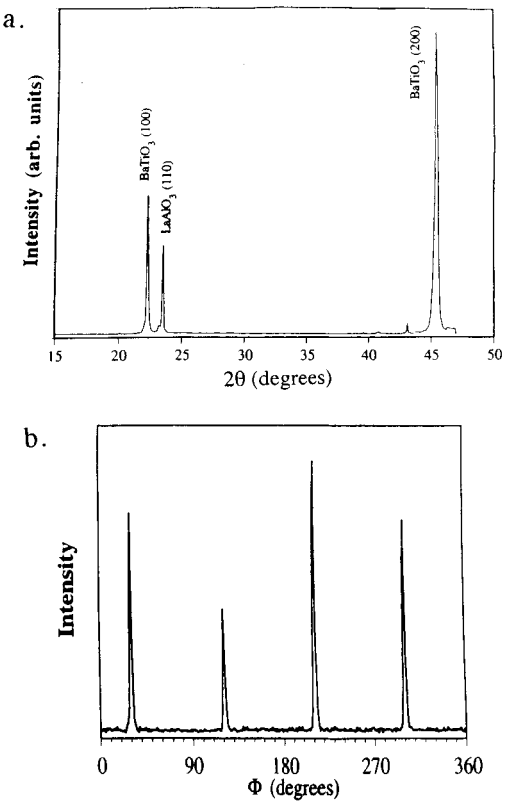

Figure 9. X-ray diffraction Θ−2Θ (a) and ϕ scans (b) of a $BaTiO_3$ thin film grown in situ on a single-crystal (110) $LaAlO_3$ substrate using complex **23** as the Ba source. The data indicate exclusive *a*-axis film orientation and in-plane epitaxy.

Conclusions

This report presents the chemical synthesis and charaterization of a broad class of $Ba(hfa)_2$·polyether complexes suitable as efficient Ba sources for oxide MOCVD film growth processes. These precursors, when compared to $Ba(dpm)_2$, offer the advantages of air and moisture stability, superior volatility, no gas-phase (or solid-state) change of molecularity (oligomerization), and ease of synthesis and handling. Furthermore, as shown here, synthetic tunability of the polyether chain, in both the terminal alkyl groups and number of ethylene oxide units, affords wide control over precursor melting point and volatility (as expressed by transport rate). Thus, we have shown that stable liquid precursors, offering the advantage of constant surface area and uniform vapor pressure, provide a sufficient, reproducible Ba flux that is suitable (and necessary) for controlled MOCVD. This result is demonstrated by the successful in situ growth of epitaxial $BaTiO_3$ thin films.

Acknowledgment. This research was supported by the NSF through the Science and Technology Center for Superconductivity (Grant DMR-9120000), the Northwestern Materials Research Center (Grant DMR 94-16926), and by NSF/ONR/ARPA (CHE-9421910/N 00014-95-1-0717). We thank the Chemistry Department at the University of Illinois, Urbana−Champaign for access to the Siemens SMART/CCD diffractometer.

Supporting Information Available: Crystallographic data for $Ba(hfa)_2$·triethyleneglycol dimethyl ether hydrate and $Ba(hfa)_2$·pentaethyleneglycol methylethyl ether (6 pages). This includes all atomic coordinates with isotropic thermal parameters, anisotropic thermal parameters, bond lengths, bond angles, and intermolecular close contact <3.20 Å for $Ba(hfa)_2$·triethyleneglycol dimethyl ether hydrate. See any current masthead page for ordering information.

CM9700108

(34) JCPDS, *Powder Diffraction Files-Inorganic Phases*, Center for Diffraction Data, Swathmore, PA, 1994.